PREPRINT

PERTANIKA JOURNALS

SCIENCE & TECHNOLOGY

Journal homepage: http://www.pertanika.upm.edu.my/

Analysis and Simulation of Temperature Reduction and Cooling Rate in Precooling Process Using Compressive Force Plate Cooler

Surya Abdul Muttalib, Nursigit Bintoro*, Joko Nugroho Wahyu Karyadi and Arifin Dwi Saputro

Department of Agricultural Engineering and Biosystem, Gadjah Mada University, 55281 Yogyakarta, Indonesia

ABSTRACT

In the precooling process of meat and fish using flaked ice, the product temperature decreases slowly due to insufficient contact between the cooling medium and the product. This study aimed to analyze the effects of meat type and compressive force level on sample temperature and cooling rate, as well as to conduct simulations using Computational Fluid Dynamics (CFD). Three types of meat samples, namely chicken, beef, and tuna fillet, were examined under three levels of compressive force: 0 N (control), 980 N, and 1960 N. The results showed that compressive force, meat type, and interaction significantly influenced the cooling rate and final sample temperature ($p<0.05$). During the initial phase of the precooling process, the average cooling rate of chicken increased by 169.2% and 391.0% compared to the control under compressive forces of 980 N and 1960 N, respectively. Similarly, the cooling rate of beef increased by 113.1% and 268.3%, while that of fish increased by 60.7% and 274.2%. The final temperatures of chicken, beef, and fish samples decreased by 41.7% and 79.0%, 22.8% and 76.0%, and 56.8% and 85.7%, respectively, under compressive forces of 980 N and 1960 N compared to the control. CFD simulations accurately predicted the final sample temperature, with an average R^2 value of 0.82, *RMSE* of 0.28, and *MAPE* of 2.33%.

Keywords: CFD simulation, compressive force, meat type, precooling

ARTICLE INFO

Article history:
Received: 25 September 2024
Accepted: 17 March 2025
Published: 11 June 2025

DOI: https://doi.org/10.47836/pjst.33.4.06

E-mail addresses:
suryaabdul2020@mail.ugm.ac.id; surya15@unram.ac.id (Surya Abdul Muttalib)
nursigit@ugm.ac.id (Nursigit Bintoro)
jknugroho@ugm.ac.id (Joko Nugroho Wahyu Karyadi)
arifin_saputro@ugm.ac.id (Arifin Dwi Saputro)
* Corresponding author

INTRODUCTION

Animal products, especially meat and fish, have a high risk of damage due to high water content and easily damaged chemicals. Red meat contains 75% water, 20% protein, 5.2% fat and 1.5% carbohydrates (Darwish et al., 2024). Proteins and fats are easily deteriorated both physiologically and enzymatically. Meanwhile, high water

e-ISSN: 2231-8526

content increases the risk of the growth of microorganisms (Merai et al., 2019; Rahman, 2007; Wang, 2000). Consequently, these products must be preserved immediately after harvest or slaughter to prevent spoilage. If meat is continuously stored at high temperatures, spoilage accelerates, leading to a decline in quality during transportation and subsequent cold chain storage. It increases the risk of foodborne diseases and reduces the product's commercial value (Han, 2014; Merai et al., 2019; Zira et al., 2021). Preservation of meat by cooling should be carried out as quickly as possible after slaughter (Merai et al., 2019; Savell et al., 2005).

Precooling is crucial for meat and fish before cold storage, as it rapidly reduces the product temperature to the required storage condition. Precooling after slaughter has become an important operational part before meat enters the cold chain (Dal et al., 2021; Ren et al., 2023). If the carcass is put directly into the cold storage room after slaughter, without precooling first, the temperature of the carcass will not be able to drop quickly to the cold storage target temperature, namely 0–4°C (Bailey et al., 2000; Chakraborty et al., 2017; El-Aal & Suliman, 2008; Merai et al., 2019; Rahman, 2007; Wang, 2000; http://www.fsis.usda.gov/search). Precooling using ice in flake or slurry has long been practiced and is very commonly used in society because it is easy to do, cheap, and does not require complicated equipment. Several researchers have used ice for the cooling process of various types of products: Li et al. (2022) for fruit and vegetables, Valtýsdóttir et al. (2010) for fish, and Gao (2007) for cod fish. However, the temperature reduction or cooling rate speed by simply covering meat or fish with ice flakes will generally be slow. Therefore, the precooling process using ice as a cooling medium needs to be improved to reduce meat temperature or increase the cooling rate. Increasing the cooling rate in this precooling method can be done by tightening the contact between the cooling ice medium and the meat by applying an external compressive force to the cooling medium. Increasing the contact intensity will increase the heat transfer rate from the meat to the cooling medium due to increasing the total heat transfer coefficient and contact surface area.

Temperature is a critical parameter in relation to product spoilage. One indicator for detecting the quality of food ingredients is temperature history (Al-Mohaithef et al., 2021; Li et al., 2019; Riva et al., 2001; Skawińska & Zalewski, 2022; Tao et al., 2023; Wang et al, 2015). CFD can provide information on the temperature history of a material being studied (Awasthi et al., 2024; Chakraborty & Dash, 2023; Chauhan et al., 2019; Cruz et al., 2022; Grossi et al., 2024; Toparlar et al., 2019; Zhang et al., 2020). Therefore, applying CFD simulations to the precooling will be very useful in providing a more comprehensive understanding of the precooling process. This research aimed to analyze the effect of meat type and compressive force on the precooling process using a compressive plate-type cooling apparatus with crushed ice as the cooling medium. In this research, CFD simulations will also be carried out to predict the final temperature of the cooled samples.

MATERIALS AND METHODS

Materials

Three types of animal products were used as research samples: beef, chicken, and tuna fillet. These samples were purchased from local markets in Yogyakarta, Indonesia. The selected meat and fish samples were fresh, unblemished, and free from any off-putting odors, representing the typical condition of meat and fish available for sale. The beef sample was tenderloin, characterized by a firm texture, bright red color, and absence of any fishy smell. The chicken meat sample was breast meat, had a dense texture, bright color, and was still fresh. Meanwhile, the tuna fish samples were fresh fish fillets with firm flesh, red gills, bright eyes, and bright fish scales that had not been peeled off. Upon arrival at the laboratory, the three types of meat samples were sliced into square shapes with dimensions of 30 mm long, 30 mm wide, and 20 mm thick. Ice was used as the cooling medium in this research. This ice was purchased from the ice supplier of ASTRA Company in Sleman, Yogyakarta, Indonesia. The ice chunks were carefully crushed into small pieces with a size of around 5 mm.

Apparatus

Figure 1(a) shows the compressive plate-type precooling apparatus constructed in this study. The primary function of this apparatus was to provide measurable pressure to the sample being tested, whose construction was made of metal. The main component of this apparatus was a mechanical pressing equipment constructed of metal. The main function of this apparatus was to compress the ice-cooling medium above the meat sample with a 10 × 10 cm stainless steel compression plate. This plate could be moved back and forth vertically using an electric motor (DC 12V, 2A, 400 rpm, torque 6.5 kg/cm). The apparatus was equipped with electronic components to monitor the compressive force and temperature of the sample and cooling medium in real time. Four K-type thermocouple sensors (model TP-01) and a loadcell sensor (capacity 500 kg, voltage 10–15V DC) were used to monitor temperatures and compressive force, respectively. Other components were the Analog Digital Converter (ADC), ATM Mega Arduino uno microcontroller (ATmega328 SMD, 5V), HX711 driver, AD8495 driver, LCD, computer, and power supply (12V, 10A). A wooden container box was used to accommodate the samples and cooling medium. This container had a thickness of 1 cm, a square base measuring 12 cm per side, and a height of 17 cm.

Research Procedures

This research began by placing crushed ice as the cooling medium along with the meat or fish fillet samples into a wooden box container. The filling process was conducted

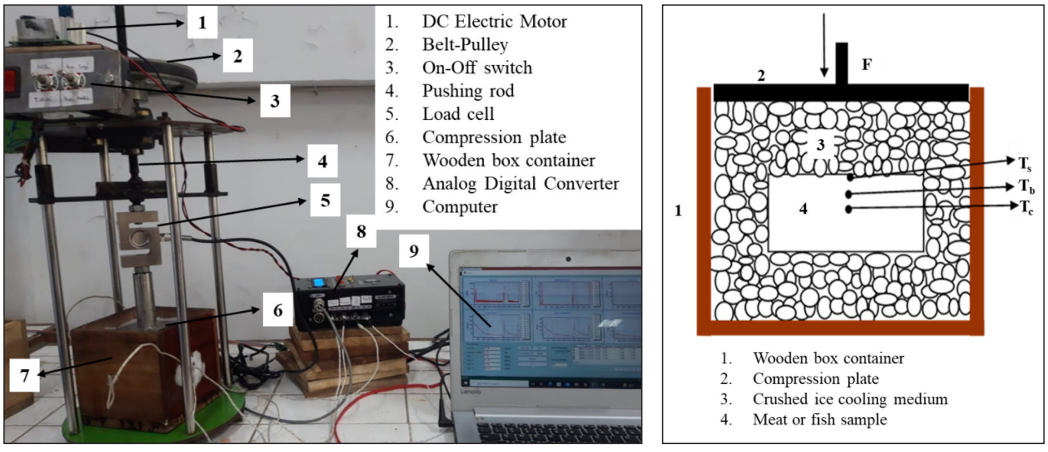

(a) (b)

Figure 1. (a) Compressive plate type precooling apparatus; and (b) schematic diagram of samples and crushed ice in the box during the precooling process

as follows: first, a 4 cm layer of crushed ice was placed at the bottom of the wooden box; next, the meat samples were positioned on top of the ice; finally, the box was filled with additional ice until it was completely full. Next, a stainless-steel compression plate was moved downward to press the cooling ice medium, as shown in Figure 1(b). The magnitude of compressive force could be adjusted according to the predetermined value by monitoring the displayed value on the computer screen. In this research, compressive forces were 0 (control), 980, and 1960 N (0, 100, and 200 kg) with a compression speed of 2 m/s. The compression would be stopped after those desired values were reached. Therefore, the meat samples were not continuously loaded with the specified compressive force during the cooling process so that the samples did not experience damage due to excessive pressure. At the same time as the force was applied to the ice, the meat sample and cooling medium temperatures were continuously monitored throughout the precooling process until the temperature of the sample being cooled reached a constant temperature. The temperature of the meat sample was measured at three positions: (1) at the center of the material (T_c), (2) at the position between the center and the surface of the material (T_b), (3) and the temperature at the surface of the material (T_s) using thermocouple sensor. Temperature data was measured every second during precooling and transferred to the computer through ADC.

Data Analysis

In this research, statistical analysis of variance (ANOVA) was used to analyze the data. The ANOVA model applied was a Completely Randomized Design (CRD), factorial 3 × 3, with three replications. The first factor was the type of meat: chicken, beef, and fish. In contrast,

the second factor was the level of compressive force applied during the precooling process, set at 0 N, 980 N, and 1960 N. Mean comparisons were evaluated using Duncan's Multiple Range Test (DMRT). According to Fiandini et al. (2023), the mean difference test was a useful tool to determine whether there were significant differences between two or more data groups. Apart from statistical analysis, simulations were also carried out to predict the final temperature of the meat sample at the three measured positions. The simulation used CFD by applying the finite element method, which was based on the natural fluid transfer of the Navier-Stokes Equation and the phenomenon of energy transfer. Fadiji et al. (2021) informed about the application of CFD in various research on freezing and thawing food products. The equations used in the CFD application program were the continuity (Equation 1), the momentum (Equation 2), and the energy (Equation 3).

$$\frac{\partial u_x}{\partial x} + \frac{\partial u_y}{\partial y} + \frac{\partial u_z}{\partial z} = 0 \quad [1]$$

$$\rho_g \frac{Dv}{Dt} = -\nabla p + \nabla \tau + \rho_g \, g \quad [2]$$

$$\frac{\partial T}{\partial t} + \mu_x \frac{\partial T}{\partial x} + \mu_y \frac{\partial T}{\partial y} + \mu_z \frac{\partial T}{\partial z} = \propto \left(\frac{\partial^2 T}{\partial x^2} + \frac{\partial^2 T}{\partial y^2} + \frac{\partial^2 T}{\partial z^2}\right) \quad [3]$$

Where u_x was the velocity in X (m/s), u_y was the velocity in Y (m/s), u_z was the velocity in Z (m/s), ρ_g was the density (kg/m^3), $\frac{Dv}{Dt}$ was derivative of volume (m^3/s), p was the pressure (Pa), μ_x was the kinematic viscosity in X (m^2/s), μ_y was the kinematic viscosity in Y (m^2/s), μ_z was the kinematic viscosity in Z (m^2/s), α was the thermal diffusivity (m^2/s), τ was the stress tensor (N/m^2), t was a time (s), g was gravitation (m/s^2), and T was the temperature (K).

Validation of simulation results was necessary to ensure that the data used and the selected model accurately represented the key aspects of the phenomenon being studied. In this research, the accuracy of simulation results in predicting measurement results was determined based on the coefficient of determination (R^2), root mean square error (*RMSE*), and mean average percentage errors (*MAPE*) calculated using Equations 4, 5, and 6, respectively.

$$R^2 = \frac{\Sigma(T_{i,obs} \; T_{i,pre})^2}{\Sigma(T_{i,obs})^2 \; \Sigma(T_{i,pre})^2} \quad [4]$$

$$RMSE = \left[\frac{1}{N}\sum_{i=1}^{N}(T_{i,obs} - T_{i,pre})^2\right]^{1/2} \quad [5]$$

$$MAPE = \sum_{i=1}^{N}\left|\frac{T_{i,obs} - T_{i,pre}}{T_{i,obs}}\right| \times 100\% \quad [6]$$

Where $T_{i,obs}$ was the measured temperature (K), $T_{i,pre}$ was the predicted temperature (K), and N was the number of data points.

RESULTS AND DISCUSSION

Cooling Rate

Figures 2, 3, and 4 show the temperature profiles of Tc, Tb, and Tc during the precooling process with the compressive force of 0, 980, and 1960 N for chicken, beef, and fish samples, respectively. It can be observed that the sample temperature consistently decreased throughout the precooling process, reaching an approximately constant temperature at around 600 seconds. The direct contact between the cooling medium and the sample surface caused the T_s value to drop more quickly. Generally, it reached a lower final temperature compared to T_b and T_c. Based on the temperature profiles, it could be observed that two patterns of temperature decrease appeared very different: (1) the initial period occurred when the compressive force began to be applied at the beginning of the precooling process until the drastic drop in sample temperature stopped at around 20 s, and (2) subsequent period, which occurred after the compressive force was stopped until the precooling process was completed. Li et al. (2022) provided an equation for calculating the cooling rate, and there was a ratio between the initial and final temperature difference and the precooling time. Therefore, based on the temperature profile of the sample, the cooling rate value could be calculated using Equations 7 and 8 for the cooling rate in the initial and subsequent periods, respectively.

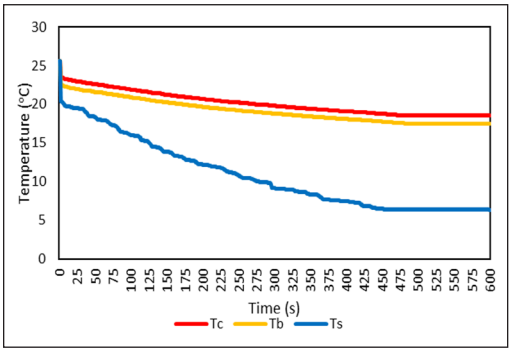

(a)

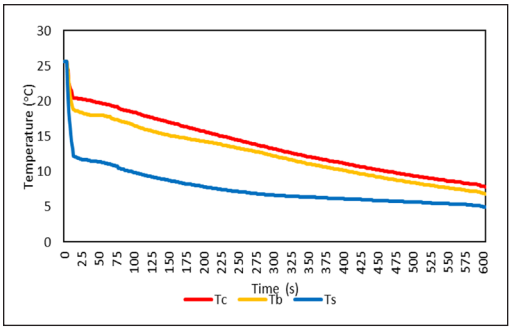

(b)

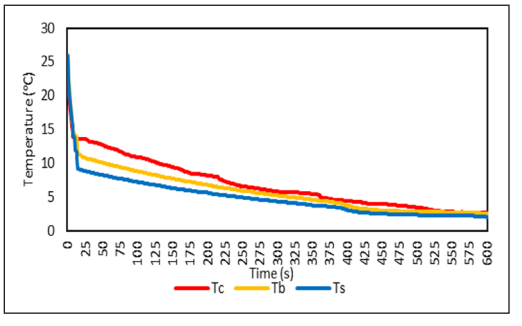

(c)

Figure 2. Temperature profile of T_c, T_b, and T_s in chicken meat samples: (a) without compressive force; (b) 980 N compressive force; and (c) 1960 N compressive force

$$CR_i = \frac{T_0 - T_i}{t_i - t_0} \quad [7]$$

$$CR_s = \frac{T_i - T_f}{t_f - t_i} \quad [8]$$

Where CR_i and CR_s were the cooling rates in the initial and subsequent periods, respectively (°C/s), T_o was the initial temperature of the material (°C), T_i was the temperature of the material at the end of the initial period (°C), T_f was the final temperature of the material when precooling was completed (°C), t_o was the initial time of the precooling process (s), t_i was the length of the initial period (s), and t_f was the length of the subsequent period (s).

Table 1 presents the cooling rate during the initial and subsequent periods and the overall average for the meat samples tested in this study. It is clearly observed that, during

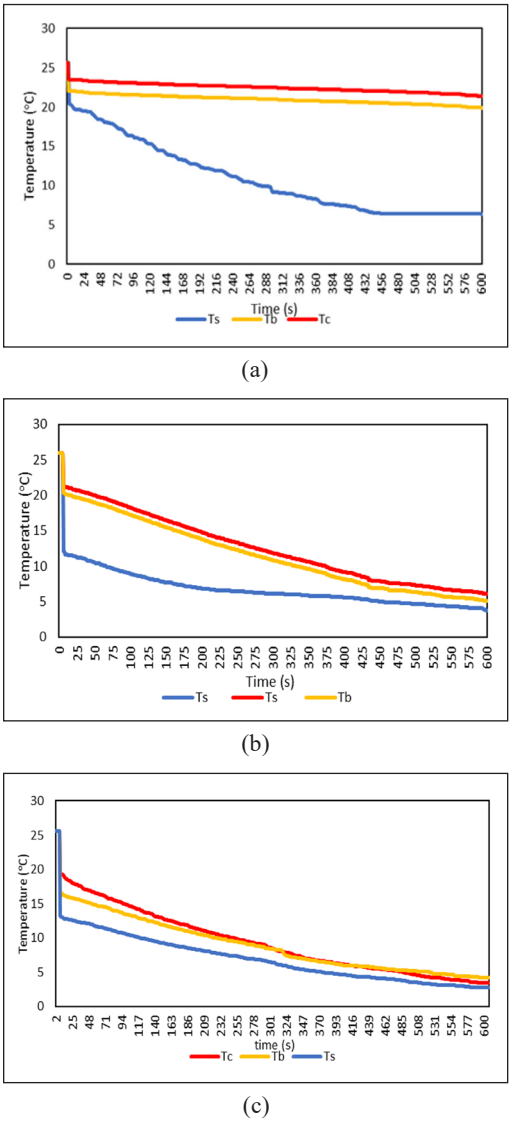

Figure 3. Temperature profile of T_c, T_b, and T_s in chicken meat samples: (a) without compressive force; (b) 980 N compressive force; and (c) 1960 N compressive force

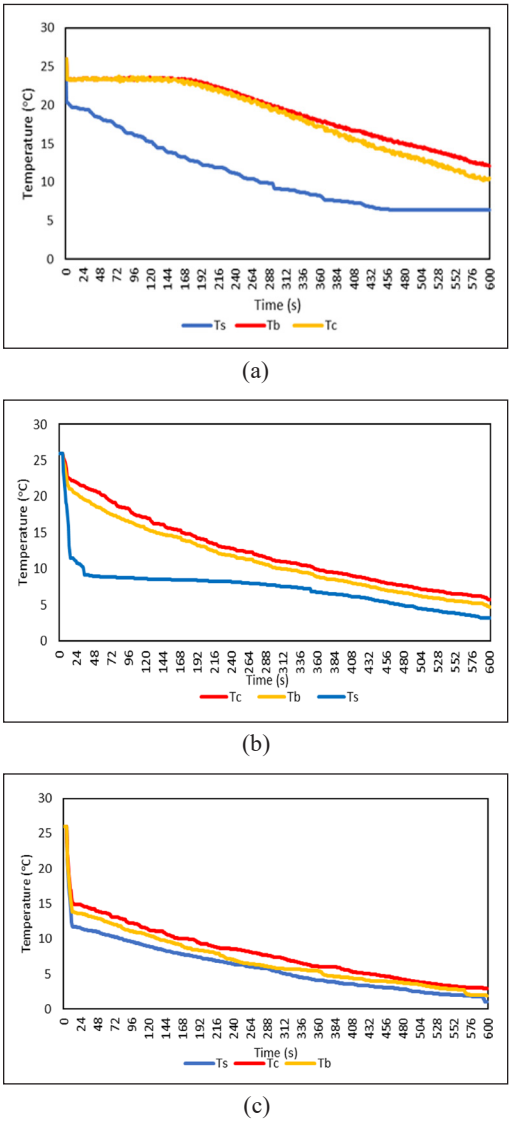

Figure 4. Temperature profile of T_c, T_b, and T_s in fish sample: (a) without compressive force; (b) 980 N compressive force; and (c) 1960 N compressive force

Table 1
The cooling rate of the meat sample (°C/s) during the precooling process.

Meat	Force (N)	Initial Period			Subsequent Period			Whole Process		
		T_s	T_b	T_c	T_s	T_b	T_c	T_s	T_b	T_c
Chicken	0	0,267^{a}	0,146^{a}	0,117^{a}	0,030^{h}	0,004^{a}	0,003^{a}	0,032^{b}	0,013^{ab}	0,012^{a}
	980	0,765^{d}	0,397^{e}	0,292^{d}	0,011^{c}	0,024^{f}	0,026^{h}	0,034^{d}	0,029^{d}	0,029^{c}
	1960	0,924^{g}	0,814^{g}	0,667^{f}	0,012^{d}	0,014^{c}	0,019^{e}	0,039^{g}	0,038^{e}	0,038^{d}
Beef	0	0,332^{b}	0,203^{b}	0,120^{a}	0,023^{g}	0,004^{a}	0,004^{b}	0,031^{a}	0,010^{a}	0,007^{a}
	980	0,778^{de}	0,306^{d}	0,304^{e}	0,007^{a}	0,008^{b}	0,008^{c}	0,033^{c}	0,018^{bc}	0,018^{c}
	1960	0,816^{f}	0,609^{f}	0,669^{f}	0,008^{b}	0,015^{b}	0,015^{e}	0,038^{f}	0,037^{e}	0,036^{d}
Fish	0	0,356^{c}	0,237^{c}	0,146^{b}	0,023^{g}	0,023^{e}	0,019^{f}	0,033^{c}	0,021^{c}	0,017^{b}
	980	0,789^{e}	0,290^{d}	0,202^{c}	0,013^{e}	0,013^{c}	0,021^{g}	0,037^{e}	0,035^{e}	0,030^{cd}
	1960	0,959^{h}	0,866^{h}	0,712^{g}	0,018^{f}	0,022^{d}	0,018^{d}	0,041^{h}	0,039^{e}	0,039^{d}

*) Numbers followed by the same letter in the column are not significantly different

the initial period, there was a drastic decrease in the temperature of the meat samples within a very short time, resulting in a high cooling rate. In contrast, during the subsequent period, the rate of temperature decrease was significantly slower, with a much lower cooling rate compared to the initial period. This condition demonstrates that applying compressive force to the cooling medium significantly enhances the cooling rate of the meat samples. The compressive force increases the heat transfer rate from the meat samples to the cooling medium by tightening the contact between them and expanding the contact surface area, thereby accelerating heat transfer (Figure 5). In the heat transfer between two media, the tighter and wider the contact surface, the overall heat transfer coefficient (U) would increase, and increasing the U value would accelerate the heat transfer process so that the product would be cooled more quickly. Muttalib et al. (2024) found that applying compressive force increased the cooling rate in the tuna fish sample. Meanwhile, in the subsequent period, when the applied compressive force was stopped, the force that had been exerted would

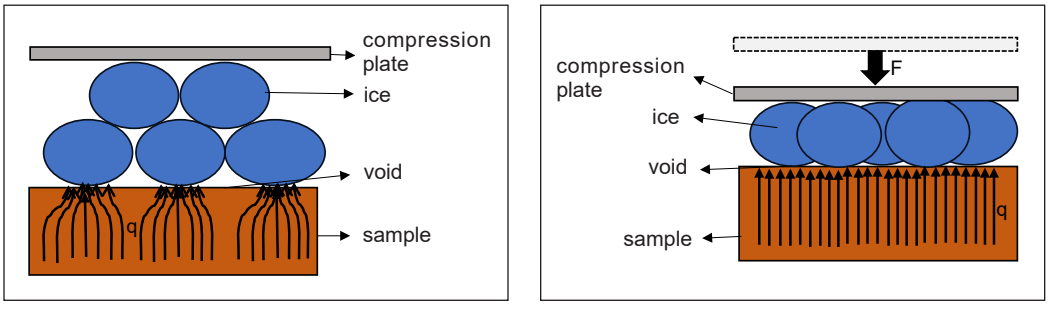

(a) (b)

Figure 5. Illustration of changes in the contact area during the precooling process: (a) without compressive force; and (b) with compressive force

gradually decrease and eventually disappear because the ice medium would absorb the force. This caused the contact between the meat samples and the ice to loosen, resulting in a much lower cooling rate and a slower temperature decrease in this phase.

It was also observed that for all types of samples, the greater the compressive force applied, the lower the temperature drop or the higher the sample cooling rate, especially in the initial period. This indicated that the greater the compressive force on the cooling medium, the faster the cooling process. In the initial period, the average cooling rate of chicken meat for the three measured locations increased by 169.2% and 391.0% compared to the control for compressive forces of 980 N and 1960 N, respectively. In this period, the cooling rate of beef increased by 113.1% and 268.3%, while the cooling rate of fish increased by 60.7% and 274.2%. During the subsequent period, the cooling rate of chicken meat increased by 385.5% and 233.8% compared to the control for compressive forces of 980 N and 1960 N, respectively. In this period, the cooling rate of beef increased by 68.6% and 195.3%; however, the cooling rate of fish was found to have no increment. For the whole precooling process, the average cooling rate of chicken meat for the three measured locations increased by 88.4% and 143.6% compared to the control for compressive forces of 980 N and 1960 N, respectively. In the same condition, the cooling rate of beef increased by 78.3% and 233.0%, while the cooling rate of fish increased by 52.0% and 80.6%. These results showed that the highest cooling rate was achieved during the initial period, with a consistent increase. Thus, the initial period was the most representative phase for evaluating the effect of compressive forces in the precooling process.

Additionally, under the same applied compressive force, the cooling rates of the three types of samples showed different values. This indicated that each type of meat had a different characteristic in the precooling process. Each type of meat had different thermal characteristics, which influenced changes in the temperature during the precooling process. One important parameter that greatly influenced the heat transfer rate from a material was the specific heat of the material (C_p). C_p represented the amount of heat required to change the temperature of 1 kg of material by 1 K. This meant that a material with a smaller C_p value would have a greater rate of decrease in material temperature because it involved changing a smaller amount of heat to change the material temperature by 1 K. The C_p values for chicken, beef, and fish were 4.34 kJ/kg K, 3.45 kJ/kg K, and 3.43 kJ/kg K, respectively (ASHRAE, 2014). Fish had the lowest C_p value among the three samples; therefore, the fish samples generally had the highest cooling rate. Fish muscles were very different from land animals such as cows and chickens. Fish muscles consisted of short fibers that were usually less than an inch long, arranged in layers called myotomes, which were separated by connective tissue called myosepta. This unique arrangement allowed the texture of the fish meat to be soft and easy to peel (Lampila, 1990). This kind of structure probably caused the fish to experience a decrease

in temperature more quickly during the cooling process. However, the difference in cooling rate between chicken and beef did not appear to be related to the C_p value, but both had lower cooling rates compared to the fish sample.

The results of statistical analysis showed that the compressive force, type of meat, and the interaction of these two factors significantly influenced the cooling rate at the center, between the center and the surface, and the surface of the sample, both in the initial and subsequent periods, as well as the whole process ($p<0.05$). Based on the DMRT results, it was generally found that meat samples subjected to compressive force exhibited higher cooling rates compared to the control. Among the samples, fish consistently showed the highest cooling rate, with the effect becoming more pronounced at higher compressive forces.

Final Sample Temperature

The final temperature of the sample, which could be achieved during the precooling process, was an important parameter for safe meat storage. In the precooling process, the desired final temperature was the temperature that was expected to be close to the storage temperature. As explained above, storage for meat and fish was generally recommended at a temperature of 4 °C (277 K) or less. Therefore, precooling using an ice medium that produced a final temperature close to this value or slightly lower would be better**.**

Table 2 presents the final temperatures of the samples during the precooling process. It was observed that the final temperature of the samples was lower when a compressive force was applied compared to the control. Furthermore, the greater the compressive force, the lower the final temperature. The final temperature of chicken, beef, and fish samples decreased by 41.7 and 79.0%, 22.8 and 76.0%, and 56.8 and 85.7% compared to the control, respectively, for applying a compressive force of 980 and 1960 N. Statistical

Table 2
The final temperature of the samples in the precooling process

Sample	Force (N)	T_s (°C)	T_b (°C)	T_c (°C)
	0	6.39^{g}	17.51^{dc}	18.51^{d}
Chicken	980	5.35^{e}	7.99^{b}	8.45^{b}
	1960	2.16^{b}	2.60^{a}	2.64^{a}
	0	7.63^{h}	19.90^{e}	21.40^{d}
Beef	980	6.37^{fg}	15.27^{cd}	15.29^{c}
	1960	2.75^{c}	3.46^{a}	3.96^{a}
	0	6.36^{f}	13.50^{c}	15.27^{c}
Fish	980	3.15^{d}	5.74^{a}	5.74^{ab}
	1960	1.04^{a}	1.97^{a}	2.96^{a}

*) Numbers followed by the same letter in the same column are not significantly different

analysis revealed that compressive force, type of meat, and the interaction of these two factors significantly influenced the final temperature of T_s, T_b, and T_c in all samples ($p<0.05$). Based on the DMRT results, in general, it could be seen that the final temperature of meat samples varied according to the force applied. The final temperature values were significantly different for different compressive forces in all meat samples. Fish samples were found to have the lowest final temperature value compared to chicken and beef. Furthermore, when applying a compressive force of 1960 N, the final temperature reached for the three samples was about the same in the range of 2°C. This was in accordance with the recommended storage requirements for meat and fish at a temperature of 4°C. Therefore, applying the compressive force of 1960 N in using a compressive plate-type cooling apparatus was a suitable choice for the precooling process of animal products for subsequent storage purposes.

CFD Simulation for Final Temperature

As mentioned earlier, in the precooling process for storage, the most critical factor is the final temperature reached by the sample material. Therefore, in this study, CFD simulations were used to predict the final temperature of T_s, T_b, and T_c of the samples. Various physical and thermal property parameters were required to run this simulation for the meat sample and the ice medium used. Table 3 shows the parameter values used in the CFD simulation in this study.

The solver used in this simulation was the Reynolds-Averaged Navier-Stokes (RANS) equation with a pressure-based, transient flow model and steady-time approach. This method was chosen because, in many engineering applications, steady flow modeling

Table 3
Parameter values used in the CFD simulation

Material	Type	Properties	Values	Sources
Crushed ice	Solid	Density (kg/m^3)	920	Ballinger et al. (2011)
		Molecular weight (kg/kmol)	18.0152	Fellows (2009)
		Specific heat (J/kg.K)	1006.43	Vernier calipers
		Thermal conductivity (W/m.K)	0.6	Thermocouple
		Average diameter (mm)	5	
		Temperature (K)	271.8	
Air	Fluid	Density (kg/m^3)	1.276	The Engineering ToolBox.
		Specific heat (J/kg.K)	1006.43	(2003)
		Thermal conductivity (W/m.K)	0.0242	Thermocouple
		Temperature (K)	271.8	
Beef	Solid	Density (kg/m^3)	1033	Hadfield (2019)
		Specific heat (J/kg.K)	3100	Fellows (2009)
		Thermal conductivity (W/m.K)	0.3	Vernier calipers
		Dimension length × width × height (mm)	30×30×20	Thermocouple
		Initial temperature (K)	298.56	

Table 3 *(continue)*

Material	Type	Properties	Values	Sources
Chicken	Solid	Density (kg/m^3)	1021	Siripon
		Specific heat (J/kg.K)	3690	Vernier calipers
		Thermal conductivity (W/m.K)	0.5	Thermocouple
		Dimension length × width × height (mm)	30×30×20	
		Initial temperature (K)	298.56	
Fish	Solid	Density (kg/m^3)	1076	Gulati & Datta, 2013;
		Specific heat (J/kg.K)	3740	Laguerre et al., 2018
		Thermal conductivity (W/m.K)	0.4	Vernier calipers
		Dimension length × width × height (mm)	30×30×20	Thermocouple
		Initial temperature (K)	298.56	

using the RANS equation is a common practice. This approach was suitable for problems where the flow field operated in quasi-steady conditions and variations over time were relatively small (Mao et al., 2020). The simulation time was designed to be the same as the actual time for the sample during the precooling process, which was 600 s. Figures 6, 7, and 8 show the final temperature contours of T_s, T_b, and T_c from the CFD simulation of the three samples at the end of precooling time, or 600 s. These results showed that CFD was able to predict the final temperature of the three samples accurately. This indicated that the tools and selected properties effectively represented the heat transfer process during precooling. The movement of heat flow from the center to the surface and towards the cooling medium was clearly depicted, indicated by clearly graded colors. The higher the temperature of any zone of the sample, the redder the color, and the lower the temperature, the bluer the color. Mixed colors from the center of the sample towards the surface indicated a zone where the temperature was changing from high to

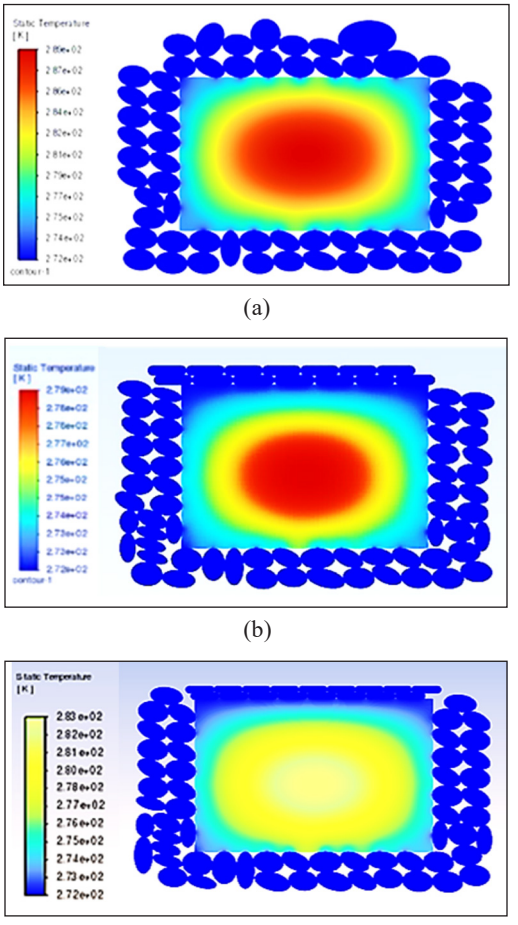

(a)

(b)

(c)

Figure 6. Temperature contour from CFD simulation for chicken meat sample: (a) without compressive force; (b) compressive force of 980 N; and (c) compressive force of 1960 N

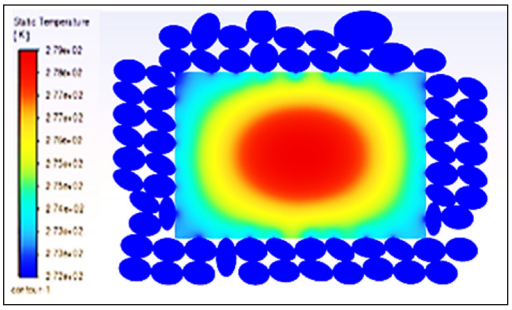

(a)

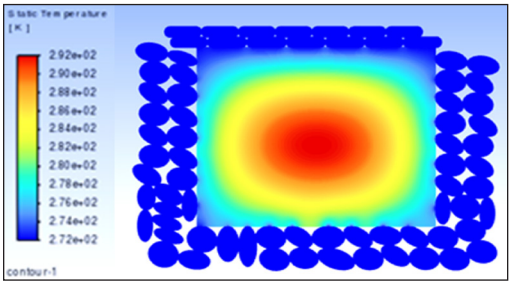

(b)

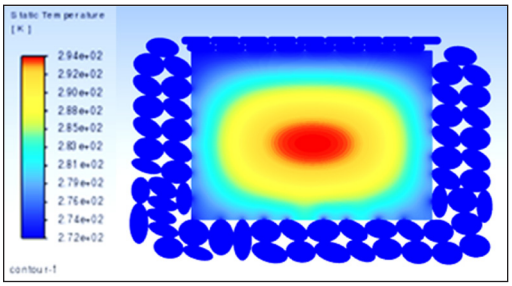

(c)

Figure 7. Temperature contour from CFD simulation for beef sample: (a) without compressive force; (b) compressive force of 980 N; and (c) compressive force of 1960 N

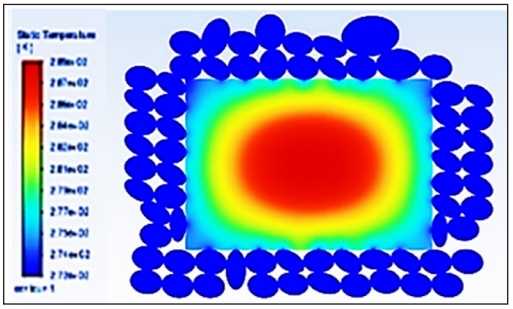

(a)

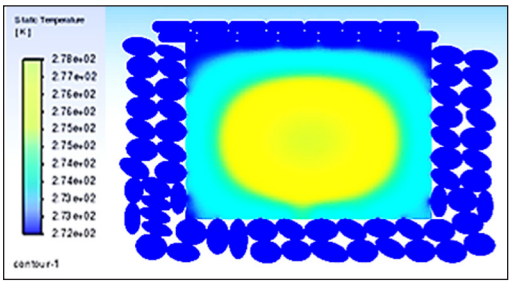

(b)

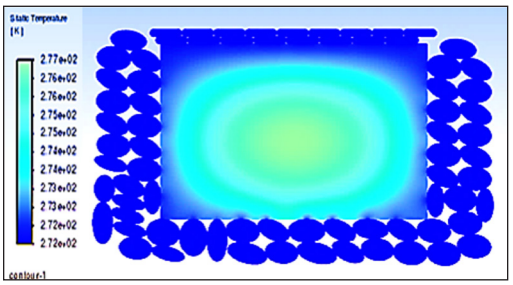

(c)

Figure 8. Temperature contour from CFD simulation for fish sample: (a) without compressive force; (b) compressive force of 980 N; and (c) compressive force of 1960 N

low. In the control treatment, the area with a reddish color, generally with a temperature of more than 280K (7°C), was the largest compared to the treatment with a compressive force of 980 or 1960 N in the three samples.

The wider reddish color indicated that high temperatures still dominated the sample temperature. At a compressive force of 980 N, the area of the reddish color became smaller, while the bluish and yellowish color at a temperature of around 275 K (2°C) to less than 280 K (7°C) became wider. This showed that with the application of compressive force, areas with high temperatures would decrease, and areas with lower temperatures would expand. At a compression force of 1960 N, the area of the reddish color at a high temperature

became smaller or disappeared, while the bluish color at a temperature of around 275K (2°C) became wider. This confirmed that the low-temperature area would dominate with a higher compressive force, indicating that the sample had a low temperature.

Table 4 presents a comparison of the final temperature of T_s, T_b, and T_c between the measurement and simulation results of the three samples, along with the R^2, *RMSE*, and *MAPE* values. In general, it could be seen that quite high R^2 values, accompanied by low RMSE and MAPE, were found at almost all measurement points and all samples tested. Overall, the predicted temperature for all measurement positions had an average R^2 value of 0.82, *RMSE* of 0.28, and *MAPE* of 2.33%. These results demonstrated that CFD

Table 4
Comparison of the final temperature of the sample from measurement and simulation, along with R^2, RMSE, and MAPE values

Sample	Measurement position	Measured	Simulated	R^2	*RMSE*	*MAPE*
Chicken (0 N)	T_s	279.39	272.58	0.69	0.44	3.39
	T_b	290.51	286.29	0.91	0.50	3.81
	T_c	291.51	282.47	0.94	0.28	1.85
Chicken (980 N)	T_s	278.35	273.26	0.93	0.29	2.28
	T_b	280.99	273.61	0.70	0.47	2.91
	T_c	281.45	282.90	0.95	0.12	0.91
Chicken (1960 N)	T_s	275.16	272.34	0.79	0.24	1.95
	T_b	275.60	273.48	0.87	0.15	2.26
	T_c	275.64	281.71	0.89	0.19	3.22
Beef (0 N)	T_s	280.63	279.07	0.94	0.06	0.40
	T_b	292.90	280.01	0.89	0.05	1.07
	T_c	294.40	289.00	0.96	0.14	0.42
Beef (980 N)	T_s	279.37	273.15	0.82	0.20	1.78
	T_b	288.27	274.36	0.61	0.36	3.01
	T_c	288.29	289.43	0.86	0.48	3.93
Beef (1960 N)	T_s	275.75	272.44	0.51	0.29	2.37
	T_b	276.46	274.49	0.73	0.21	1.69
	T_c	276.96	288.39	0.85	0.55	4.75
Fish (0 N)	T_s	279.36	272.26	0.78	0.29	2.26
	T_b	286.5	274.77	0.73	0.42	3.85
	T_c	288.27	278.68	0.98	0.06	0.33
Fish (980 N)	T_s	276.15	272.58	0.85	0.19	2.53
	T_b	278.74	272.81	0.68	0.38	3.11
	T_c	278.74	278.97	0.88	0.30	1.64
Fish (1960 N)	T_s	274.04	272.11	0.77	0.26	2.15
	T_b	274.97	272.91	0.80	0.17	1.38
	T_c	275.96	277.98	0.84	0.45	3.72

accurately predicted the sample temperatures during the precooling process, reinforcing earlier findings. CFD has proven to be a valuable tool for the food processing industry in various fields (Anandharamakrishnan et al., 2009; Bhargava et al., 2021; Oyinloye & Yoon, 2021; Padhi, 2020; Park & Yoon, 2018; Szpicer et al., 2023; Xia & Sun, 2002). There was a slightly greater deviation, especially for the final temperature at the surface position. The movement of the ice medium during compression allowed the temperature on the surface of the sample to become unstable. Kuffi et al. (2016) stated that the temperature prediction results using CFD were in accordance with the temperature profile measured at various positions on the beef carcass, with very good predictions in the deep rear position compared to the near-surface position.

CONCLUSION

It was found that compressive force, meat type, and their interaction significantly influenced the cooling rate and final temperature at all measurement positions for all sample types ($p<0.05$). Applying a compressive force in the precooling process sped up temperature reduction and increased the cooling rate of the sample.

At the initial period of the precooling process, the cooling rate reached the highest value and increased consistently. This period best represented the effect of applying compressive forces in the precooling process. In this initial period, the average cooling rate of chicken meat increased by 169.2% and 391.0% compared to the control for compressive forces of 980 N and 1960 N, respectively. Meanwhile, the cooling rate of beef increased by 113.1% and 268.3%, and the cooling rate of fish increased by 60.7% and 274.2%.

The final temperature of chicken, beef, and fish samples decreased by 41.7% and 79.0%, 22.8% and 76.0%, and 56.8% and 85.7%, respectively, compared to the control when applying a compressive force of 980 N and 1960 N. CFD simulations could accurately predict the final temperature of the samples in the precooling process, with an average R^2 value of 0.82, *RMSE* of 0.28, and *MAPE* of 2.33%.

ACKNOWLEDGMENTS

The authors thank Gadjah Mada University for partially funding this research through the Final Assignment Recognition Program (Program Rekognisi Tugas Akhir, RTA) with assignment letter No.: 5286/UN1.P1/PT.01.03/2024.

REFERENCES

Al-Mohaithef, M., Abidi, S. T., Javed, N. B., Alruwaili, M., & Abdelwahed, A. Y. (2021). Knowledge of safe food temperature among restaurant supervisors in Dammam, Saudi Arabia. *Journal of Food Quality*, *2021*, 1–8. https://doi.org/10.1155/2021/2231371

Anandharamakrishnan, C., Gimbun, J., Stapley, A. G. F., & Rielly, C. D. (2009). Application of computational fluid dynamics (CFD) simulations to spray-freezing operations. *Drying Technology*, *28*(1), 94–102. https://doi.org/10.1080/07373930903430843

ASHRAE. (2014). *ASHRAE® Handbook-Refrigeration.* ASHRAE. https://azaranstore.com/wp-content/uploads/2022/09/271-ASHRAE-HANDBOOK-REFRIGERATION-2014.pdf

Awasthi, M. K., Kumar, A., Dutt, N., & Singh, S. (2024). *Computational Fluid Flow and Heat Transfer: Advances, Design, Control, and Applications* (1st ed.). CRC Press. https://doi.org/10.1201/9781003465171

Bailey, J. M., Dunne, M. P., & Martin, N. G. (2000). Genetic and environmental influences on sexual orientation and its correlates in an Australian twin sample. *Journal of Personality and Social Psychology*, *78*(3), 524–536. https://doi.org/10.1037/0022-3514.78.3.524

Ballinger, J. T., Shugar, G. J., Ballinger, C. T., & Shugar, G. J. (2011). *Chemical technicians' ready reference handbook* (5th ed). McGraw-Hill.

Bhargava, N., Mor, R. S., Kumar, K., & Sharanagat, V. S. (2021). Advances in application of ultrasound in food processing: A review. *Ultrasonics Sonochemistry*, *70*, Article 105293. https://doi.org/10.1016/j.ultsonch.2020.105293

Chakraborty, A., Lyonnais, S., Battistini, F., Hospital, A., Medici, G., Prohens, R., Orozco, M., Vilardell, J., & Solà, M. (2017). DNA structure directs positioning of the mitochondrial genome packaging protein Abf2p. *Nucleic Acids Research*, *45*(2), 951–967. https://doi.org/10.1093/nar/gkw1147

Chakraborty, S., & Dash, K. K. (2023). A comprehensive review on heat and mass transfer simulation and measurement module during the baking process. *Applied Food Research*, *3*(1), Article 100270. https://doi.org/10.1016/j.afres.2023.100270

Chauhan, A., Trembley, J., Wrobel, L. C., & Jouhara, H. (2019). Experimental and CFD validation of the thermal performance of a cryogenic batch freezer with the effect of loading. *Energy*, *171*, 77–94. https://doi.org/10.1016/j.energy.2018.12.149

Cruz, P. A. D., Yamat, E. J. E., Nuqui, J. P. E., & Soriano, A. N. (2022). Computational fluid dynamics (CFD) analysis of the heat transfer and fluid flow of copper (II) oxide-water nanofluid in a shell and tube heat exchanger. *Digital Chemical Engineering*, *3*, Article 100014. https://doi.org/10.1016/j.dche.2022.100014

Darwish, W. S., El Bayoumi, R. M., Mohamed, N. H., & Hussein, M. A. M. (2024). Microbial contamination of meat at a low temperature storage: A review. *Journal of Advanced Veterinary Research, 14*(2), 322-325.

Dal, H. O. G., Gursoy, O., & Yilmaz, Y. (2021). Use of ultrasound as a pre-treatment for vacuum cooling process of cooked broiler breasts. *Ultrasonics Sonochemistry*, *70*, Article 105349. https://doi.org/10.1016/j.ultsonch.2020.105349

El-Aal, A., & Suliman, A. I. A. (2008). Carcass traits and meat quality of lamb fed on ration containing different levels of leucaena hay (*Leucaena leucocephala* L.). *Biotechnology in Animal Husbandry*, *24*(3–4), 77–92. https://doi.org/10.2298/BAH0804077E

Fadiji, T., Ashtiani, S. H. M., Onwude, D. I., Li, Z., & Opara, U. L. (2021). Finite element method for freezing and thawing industrial food processes. *Foods*, *10*(4), Article 869. https://doi.org/10.3390/foods10040869

Fellows, P. J. (2009). Heat processing. In *Food Processing Technology: Principles and Practice* (pp. 339-366). Woodhead Publishing.

Fiandini, M., Nandiyanto, A. B. D., Al Husaeni, D. F., Al Husaeni, D. N., & Mushiban, M. (2023). How to calculate statistics for significant difference test using SPSS: Understanding students comprehension on the concept of steam engines as power plant. *Indonesian Journal of Science and Technology*, *9*(1), 45–108. https://doi.org/10.17509/ijost.v9i1.64035

Gao, H. Y. (2007). *Methods of Pre-Cooling for Fresh Cod (Gadus morhua) and Influences on Quality during Chilled Storage at -1.5˚c*. UNU - Fisheries Training Programme.

Grossi, G., Arpino, F., Canale, C., Cortellessa, G., Ficco, G., & Lombardi, T. (2024). CFD design of a novel device for temperature profile measurement in waste-to-energy plants. *Journal of Physics: Conference Series*, *2685*(1), Article 012011. https://doi.org/10.1088/1742-6596/2685/1/012011

Gulati, T., & Datta, A. K. (2013). Enabling computer-aided food process engineering: Property estimation equations for transport phenomena-based models. *Journal of Food Engineering*, *116*(2), 483–504. https://doi.org/10.1016/j.jfoodeng.2012.12.016

Hadfield, J. M. (2019). *The thermal and physical properties of beef from three USDA-quality grades cooked to multiple degrees of doneness* [Master thesis, Utah State University]. ProQuest. https://www.proquest.com/openview/76811deb147da19bbc2df6b96cb5bbbc/1?cbl=18750&diss=y&pq-origsite=gscholar

Han, J. H. (2014). *Innovations in food packaging* (2nd ed.). Academic Press.

Kuffi, K. D., Defraeye, T., Nicolai, B. M., De Smet, S., Geeraerd, A., & Verboven, P. (2016). CFD modeling of industrial cooling of large beef carcasses. *International Journal of Refrigeration*, *69*, 324–339. https://doi.org/10.1016/j.ijrefrig.2016.06.013

Laguerre, O., Derens, E., & Flick, D. (2018). Modelling of fish refrigeration using flake ice. *International Journal of Refrigeration*, *85*, 97–108. https://doi.org/10.1016/j.ijrefrig.2017.09.014

Lampila, L. E. (1990). Comparative microstructure of red meat, poultry and fish muscle. *Journal of Muscle Foods*, *1*(4), 247–267. https://doi.org/10.1111/j.1745-4573.1990.tb00369.x

Li, Q., Duan, M., Liu, W., Dai, Y., & Li, R. (2019). Kinetic modeling of a Bi-enzyme time-temperature indicator (TTI) based on different parameters for monitoring food product quality. In *IOP Conference Series: Materials Science and Engineering* (Vol. 612, No. 2, p. 022042). IOP Publishing. https://doi.org/10.1088/1757-899X/612/2/022042

Li, X., Wu, W., Li, K., Ren, X., & Wang, Z. (2022). Experimental study on a wet precooling system for fruit and vegetables with ice slurry. *International Journal of Refrigeration*, *133*, 9–18. https://doi.org/10.1016/j.ijrefrig.2021.10.001

Mao, J., Zhao, L., Di, Y., Liu, X., & Xu, W. (2020). A resolved CFD–DEM approach for the simulation of landslides and impulse waves. *Computer Methods in Applied Mechanics and Engineering*, *359*, Article 112750. https://doi.org/10.1016/j.cma.2019.112750

Merai, M., Flick, D., Guillier, L., Duret, S., & Laguerre, O. (2019). Experimental characterization of heat transfer inside a refrigerated trailer loaded with carcasses. *International Journal of Refrigeration*, *99*, 194–203. https://doi.org/10.1016/j.ijrefrig.2018.11.041

Muttalib, S. A., Bintoro, N., Karyadi, J. N. W., & Saputro, A. D. (2024). Development of method and apparatus to speed up cooling process of fish products. In *AIP Conference Proceedings* (Vol. 2838, No. 1). AIP Publishing. https://doi.org/10.1063/5.0180090

Oyinloye, T., & Yoon, W. (2021). Application of computational fluid dynamics (CFD) simulation for the effective design of food 3D printing (A Review). *Processes*, *9*(11), Article 1867. https://doi.org/10.3390/pr9111867

Padhi, M. R. (2020). A review on applications of computational fluid dynamics (CFD) in the food industry. *PalArch's Journal of Archaeology of Egypt / Egyptology, 17*, 10159-10169

Park, H. W., & Yoon, W. B. (2018). Computational fluid dynamics (CFD) modelling and application for sterilization of foods: A review. *Processes*, *6*(6), Article 62. https://doi.org/10.3390/pr6060062

Rahman, S. (Ed.). (2007). *Handbook of food preservation* (2nd ed). CRC Press.

Ren, Q., Zhu, X., Li, J., Han, J., & Fang, K. (2023). Heat and mass transfer model for pork carcass precooling: Comprehensive evaluation and optimization. *Food and Bioproducts Processing*, *138*, 70–85. https://doi.org/10.1016/j.fbp.2023.01.004

Riva, M., Piergiovanni, L., & Schiraldi, A. (2001). Performances of time–temperature indicators in the study of temperature exposure of packaged fresh foods. *Packaging Technology and Science*, *14*(1), 1–9. https://doi.org/10.1002/pts.521

Savell, J. W., Mueller, S. L., & Baird, B. E. (2005). The chilling of carcasses. *Meat Science*, *70*(3), 449–459. https://doi.org/10.1016/j.meatsci.2004.06.027

Siripon, K., Tansakul, A., & Mittal, G.S. (2007). Heat transfer modeling of chicken cooking in hot water. *Food Research International, 40*(7), 923-930. https://doi.org/10.1016/j.foodres.2007.03.005

Skawińska, E., & Zalewski, R. I. (2022). Economic impact of temperature control during food transportation - A COVID-19 perspective. *Foods*, *11*(3), Article 467. https://doi.org/10.3390/foods11030467

Szpicer, A., Bińkowska, W., Wojtasik-Kalinowska, I., Salih, S. M., & Półtorak, A. (2023). Application of computational fluid dynamics simulations in food industry. *European Food Research and Technology*, *249*(6), 1411–1430. https://doi.org/10.1007/s00217-023-04231-y

Tao, Y., Guo, Y., Li, J., Ye, K., Zhang, Y., Zeng, X., & Dou, H. (2023). Effect of temperature fluctuation during superchilling storage on the microstructure and quality of raw pork. *Meat Science*, *198*, Article 109096. https://doi.org/10.1016/j.meatsci.2023.109096

The Engineering ToolBox (2009). *Air Psychrometrics*. https://www.engineeringtoolbox.com/air-psychrometrics-properties-t_8.html

Toparlar, Y., Blocken, B., Maiheu, B., & Van Heijst, G. (2019). CFD simulation of the near-neutral atmospheric boundary layer: New temperature inlet profile consistent with wall functions. *Journal of Wind Engineering and Industrial Aerodynamics*, *191*, 91–102. https://doi.org/10.1016/j.jweia.2019.05.016

Valtýsdóttir, K. L., Margeirsson, B., Arason, S., Lauzon, H. L., & Martinsdóttir, E. (2010). *Guidelines for Precooling of Fresh Fish during Processing and Choice of Packaging with Respect to Temperature Control in Cold Chains*. Matís. https://kaeligatt.matis.is/wp-content/uploads/2023/02/40-10-Guidelines-for-precooling-and-packaging.pdf

Wang, S. K. (2000). *Handbook of air conditioning and refrigeration* (2nd ed). McGraw-Hill.

Wang, S., Liu, X., Yang, M., Zhang, Y., Xiang, K., & Tang, R. (2015). Review of time temperature indicators as quality monitors in food packaging. *Packaging Technology and Science, 28*, 839-867. https://doi: 10.1002/pts.2148

Xia, B., & Sun, D. W. (2002). Applications of computational fluid dynamics (CFD) in the food industry: A review. *Computers and Electronics in Agriculture*, *34*(1–3), 5–24. https://doi.org/10.1016/S0168-1699(01)00177-6

Zhang, X., Ge, Y., & Sun, J. (2020). CFD performance analysis of finned-tube CO_2 gas coolers with various inlet air flow patterns. *Energy and Built Environment*, *1*(3), 233–241. https://doi.org/10.1016/j.enbenv.2020.02.004

Zira, S., Rydhmer, L., Ivarsson, E., Hoffmann, R., & Röös, E. (2021). A life cycle sustainability assessment of organic and conventional pork supply chains in Sweden. *Sustainable Production and Consumption*, *28*, 21–38. https://doi.org/10.1016/j.spc.2021.03.028